United States Department of Commerce
Technology Administration
National Institute of Standards and Technology

NISTIR 5032

Electromagnetic Shielding Characterization of Gaskets

David A. Hill

NISTIR 5032

Electromagnetic Shielding Characterization of Gaskets

David A. Hill

Electromagnetic Fields Division
Electronics and Electrical Engineering Laboratory
National Institute of Standards and Technology
Boulder, Colorado 80303-3328

February 1995

U.S. DEPARTMENT OF COMMERCE, Ronald H. Brown, Secretary
TECHNOLOGY ADMINISTRATION, Mary L. Good, Under Secretary for Technology
NATIONAL INSTITUTE OF STANDARDS AND TECHNOLOGY, Arati Prabhakar, Director

CONTENTS

Page

Abstract....1

1. INTRODUCTION....1

2. TWO-DIMENSIONAL MODEL....2
   2.1 Analytical Results....2
   2.2 Transfer Impedance....6
   2.3 Shielding Effectiveness....9

3. SLOTS OF FINITE LENGTH....10
   3.1 Short Slots....10
   3.2 Long Slots....12

4. GASKET MEASUREMENTS....15
   4.1 Measurement Geometries....15
   4.2 Measured Data....16

5. CONCLUSIONS AND RECOMMENDATIONS....19

6. REFERENCES....20

ELECTROMAGNETIC SHIELDING CHARACTERIZATION OF GASKETS

David A. Hill

Electromagnetic Fields Division
National Institute of Standards and Technology
Boulder, Colorado 80303

Numerous measurement methods are used for determining the shielding performance of rf gaskets, but different methods give significantly different results for the same gasket. Various measurement methods and the reasons for the discrepancies are reviewed. Simple models and theories are used to explain the meaning of transfer impedance and shielding effectiveness for gaskets and to determine the frequency range of validity. Transfer impedance should be a valid characterization at low frequencies, and shielding effectiveness is more appropriate at high frequencies. The precise frequency limitations of these characterizations and current measurement methods are not well known, but a time-domain method is proposed for determining gasket properties over a broad frequency range.

Key words: coaxial fixture; gasket; reverberation chamber; shielded room; shielding effectiveness; slot; transfer impedance.

1. INTRODUCTION

Numerous gasket materials are used for a broad range of electromagnetic shielding applications. Several measurement techniques [1-4] are available for determining the shielding performance of gaskets, but discrepancies have been reported in the the results obtained with the different techniques [5]. Discrepancies are not surprising since different techniques use different fixtures and in some cases measure different quantities. Transfer impedance [3,6] and shielding effectiveness (SE) [1,2,4] are the two commonly used measures of gasket shielding performance.

The purpose of this report is to review the theory of slots and gaskets with the goal of efficient characterization and measurement of gasket performance. Many gaskets are complex, inhomogeneous structures, but for

characterization we will restrict our analysis to simple models with a small number of parameters.

The organization of this report is as follows. Section 2 uses the two-dimensional model of Harrington and Aukland [7] to characterize a lossy gasket in a thick slot. Expressions are derived for both transfer impedance and shielding effectiveness. Section 3 deals with gaskets of finite length. Short gaskets can be described by a deterministic theory, but long gaskets are best described by a statistical theory which is compatible with the reverberation chamber measurement technique [2]. Section 4 presents a review of measurement geometries and a qualitative comparison of measured data and theory. Section 5 contains conclusions and recommendations for further experimental and theoretical work.

2. TWO-DIMENSIONAL MODEL

The problem of transmission through a slot in a conducting screen has been analyzed by several methods (see [8] for a bibliography). The formulation in [7] is particularly useful because it provides analytical results and allows for the presence of a lossy material (gasket) in the slot. The restriction that the slot is narrow is satisfied for most practical cases of interest. The physical significance of the two-dimensional model will be discussed in following sections.

2.1 Analytical Results

In this section we review the results of [7] and derive some related results of special interest. In most cases we retain the notation in [7]. The two-dimensional geometry for a slot in a thick screen is shown in figure 1. The source is in region a, and region c is the shielded region. The formulation in [7] allows for different constitutive parameters in regions a and c, but for simplicity we assume that both regions are free space with permittivity ϵ_0 and permeability μ_0. Region b (gasket) has permittivity ϵ_b and permeability μ_b, and both can be complex to include electric or magnetic

loss. The perfectly conducting screen has thickness d, and the slot has width w.

For narrow slots in thick conductors, only the TE (electric field transverse to the slot direction z) polarization can penetrate the slot. Consequently, the TM case will not be considered here. For TE polarization, the nonzero field components are H_z, E_x, and E_y. The excitation can be either a radiated field or a conducted current, but in either case the problem can be formulated in terms of the short-circuit surface current density which has only a y component J_y^{sc}. The short-circuit magnetic field has only a z component H_z^{sc}:

$$H_z^{sc} = J_y^{sc}. \tag{1}$$

The impressed current density J^i is the short-circuit current density averaged over the slot width:

$$J^i = \frac{1}{w} \int_0^w J_y^{sc} \, dy. \tag{2}$$

(Harrington and Aukland [7] use I^i, but we choose J^i to indicate that it is a surface current density with units of A/m.)

For the case of a normally incident plane wave, the incident magnetic field H_z^{i0} in region a is

$$H_z^{i0} = H_0 \, e^{-jk_0 x}, \tag{3}$$

where $k_0 = \omega(\mu_0 \epsilon_0)^{1/2}$ and the time dependence is $\exp(j\omega t)$. H_0 is a constant, and the short-circuit magnetic field and current are twice the incident magnetic field:

$$H_z^{sc} = J_y^{sc} = 2H_0. \tag{4}$$

The power P_{inc} incident on the aperture (per unit length) is

$$P_{inc} = \eta_0 |H_0|^2 w, \tag{5}$$

where $\eta_0 = (\mu_0/\epsilon_0)^{1/2}$.

The admittance treatment in [7] is described by the equivalent circuit in figure 2. The TEM transmission line section of length d has characteristic admittance Y_0 and wavenumber k_b given by

$$Y_0 = 1/(w\eta_b) \text{ and } k_b = \omega(\mu_b\epsilon_b)^{1/2}, \tag{6}$$

where $\eta_b = (\mu_b/\epsilon_b)^{1/2}$. The elements of the two-port admittance matrix for the transmission line section are given by

$$Y_{11}^b = Y_{22}^b = -jY_0 \cot(k_b d)$$

and (7)

$$Y_{12}^b = Y_{21}^b = jY_0 \csc(k_b d).$$

(The expression for Y_{12}^b and Y_{21}^b in [7] has a typographical sign error.) The aperture admittances opening into regions a and c are given by

$$Y^a = Y^c = \frac{1}{\eta_0 \lambda_0} [\pi - 2j \ln(Ck_0 w)], \tag{8}$$

where $C \approx 0.2226$ and λ_0 is the free-space wavelength. The network equations of the equivalent circuit in figure 2 are

$$Y^a V_1 + Y_{11}^b V_1 + Y_{12}^b V_2 = J^i$$

and (9)

$$Y_{21}^b V_1 + Y_{22}^b V_2 + Y^c V_2 = 0,$$

where V_1 is the slot voltage at $x = 0$ and V_2 is the slot voltage at $x = d$.

For gasket applications, the transfer admittance Y_{12} is of interest and can be obtained from eqs (7) and (9):

$$Y_{12} = \frac{J^i}{V_2} = (Y^a + Y^c)\cos(k_b d) + j\left(Y_0 + \frac{Y^a Y^c}{Y_0}\right)\sin(k_b d). \tag{10}$$

The input admittance Y_{11} is also of interest and can also be obtained from eqs (7) and (9):

$$Y_{11} = \frac{J^i}{V_1} = Y^a - jY_0\cot(k_b d) + \frac{Y_0^2 \csc^2(k_b d)}{Y^c - jY_0\cot(k_b d)}. \tag{11}$$

Both Y_{11} and Y_{12} are really admittances per unit length with units of S/m. The power (per unit length) transmitted through the slot is equal to that dissipated in Y^c in figure 2 and is given by

$$P_{trans} = |V_2|^2 \, \mathrm{Re}(Y^c) = |J^i/Y_{12}|^2 \, \mathrm{Re}(Y^c). \tag{12}$$

Equations (10)-(12) contain both Y^a and Y^c even though they have been assumed equal in eq (8). The preservation of both quantities allows the reader to determine which region (a or c) affects the various factors.

2.2 Transfer Impedance

For realistic three-dimensional geometries, the transfer impedance [3,6] is normally defined as a voltage/current ratio with units of Ω. In section 3, we will discuss slots of finite length. However, the two-dimensional geometry is simple and is useful for examining the dependence on all parameters except slot length.

If we define a transfer impedance Z_{t2} for the two-dimensional case as the ratio of voltage to current density, then it is determined from eq (10):

$$Z_{t2} = V_2/J^i = 1/Y_{12}. \tag{13}$$

Similarly, we can define an input impedance Z_2:

$$Z_2 = V_1/J^i = 1/Y_{11}. \tag{14}$$

Both Z_{t2} and Z_2 have units of Ω•m. In general Z_{t2} and Z_2 have complicated frequency dependence because Y_{12} and Y_{11} include several terms. However, we can examine special cases where eqs (13) and (14) simplify.

Consider the case where $|k_b|d \ll 1$. This condition could be thought of as a low-frequency condition where it is also reasonable to assume that $|Y_0|^2 \gg |Y^a Y^c|$. Then we can approximate Z_{t2} by

$$Z_{t2} \approx (Y^a + Y^c + jk_b dY_0)^{-1}. \tag{15}$$

The form in eq (15) is consistent with [9, p. 513] which applies to general geometries where Y^a and Y^c can be different. If we neglect the first two terms in eq (15), then Z_{t2} can be further approximated as

$$Z_{t2} \approx \frac{w}{j\omega\epsilon_b d}. \tag{16}$$

For a highly conducting gasket material, the conduction currents dominate the displacement currents, and the complex dielectric constant can be written

$$\epsilon_b \approx \frac{\sigma_b}{j\omega}. \tag{17}$$

If we substitute eq (17) into eq (16), we obtain the expected dc limit

$$Z_{t2} \approx \frac{w}{\sigma_b d}. \tag{18}$$

As the gasket conductivity σ_b approaches ∞, the transfer impedance and the slot voltage V_2 approach 0. The same approximations can be made for Z_2 to yield the same result

$$Z_2 \approx \frac{w}{\sigma_b d}. \tag{19}$$

The high-frequency case where $|k_b|d >> 1$ is also of interest. If we assume that k_b is complex due to loss, then we can approximate the trigonometric functions in eq (10):

$$\cos(k_b d) \approx j\sin(k_b d) \approx \frac{1}{2} e^{jk_b d}. \tag{20}$$

The transfer impedance is then approximated by

$$Z_{t2} \approx 2[Y^a + Y^c + Y_0 + \frac{Y^a Y^c}{Y_0}]^{-1} e^{-jk_b d}. \tag{21}$$

The exponential factor in eq (21) represents the one-way attenuation and phase shift in the gasket region. If $|Y_0| >> |Y^a|$, then eq (21) reduces to

$$Z_{t2} \approx 2w\eta_b \, e^{-jk_b d} . \tag{22}$$

If conduction currents dominate and ϵ_b can be approximated by eq (17), then Z_{t2} can be further approximated as

$$Z_{t2} \approx 2w \left(\frac{j\omega\mu_b}{\sigma_b}\right)^{1/2} e^{-(j\omega\mu_b\sigma_b)^{1/2}d} . \tag{23}$$

The exponential factor yields the standard skin-depth attenuation and phase shift. If the same approximations are made in Z_2, the result is

$$Z_2 \approx w \left(\frac{j\omega\mu_b}{\sigma_b}\right)^{1/2} . \tag{24}$$

The previous results in eqs (15)-(24) apply to a lossy material that completely fills the slot. Another case of interest is a highly conducting gasket that makes imperfect contact with the slot walls and leaves a thin air gap. This case can be studied from the figure 1 model by setting $\epsilon_b = \epsilon_0$ and $\mu_b = \mu_0$ and assuming $k_0 w$ and $k_0 d << 1$. Then Z_{t2} can be approximated by

$$Z_{t2} \approx \frac{j2\pi\eta_0}{k_0 \, \ell n(k_0 w)} . \tag{25}$$

This case yields a slow decrease in $|Z_{t2}|$ with frequency.

2.3 Shielding Effectiveness

Shielding effectiveness (SE) is normally defined as the insertion loss of the shield or in this case the gasket. Since the slot radiates like a magnetic line source whether or not the gasket is present, the shape of the radiated pattern is not affected by the gasket. The strength of the z-directed magnetic line current K located at x = d is equal to the slot voltage V_2. The total power radiated into region c is given by eq (12).

SE in dB can be written

$$SE = 10 \log_{10}(P_{trans,0}/P_{trans,g}), \text{ dB}, \tag{26}$$

where $P_{trans,0}$ is the power transmitted in the absence of the gasket ($\epsilon_b = \epsilon_0$, $\mu_b = \mu_0$) and $P_{trans,g}$ is the power transmitted with the gasket in place. From eqs (12) and (26), we can write SE as

$$SE = 20 \log_{10}(|Y_{12,g}/Y_{12,0}|), \text{ dB}, \tag{27}$$

where $Y_{12,0}$ is the transfer admittance, given by eq (12), in the absence of the gasket and $Y_{12,g}$ is the transfer admittance with the gasket in place. By using eqs (13) and (27), we can also write SE in terms of the transfer impedances:

$$SE = 20 \log_{10}(|Z_{t2,0}/Z_{t2,g}|), \text{ dB}, \tag{28}$$

where the subscripts 0 and g again refer to the absence and presence of the gasket. As $|Z_{t2,g}|$ approaches 0, SE approaches ∞.

3. SLOTS OF FINITE LENGTH

For slots and gaskets of finite length, the problem becomes more complicated because the current density and slot voltage are not necessarily constant along the slot. Integral equation methods [10-13] can be used to solve for the slot voltage as a function of position, but we will not pursue these methods here.

3.1 Short Slots

In this section we consider slots whose widths are comparable to or smaller than the free-space wavelength. Then, it is convenient to define a transfer impedance Z_t with units of Ω as a voltage-current ratio:

$$Z_t = V_2/I^i, \tag{29}$$

where I^i is the total current in the absence of the slot. The potential difficulty is that the voltage V_2 can be a function of position along the slot.

Equation (29) applies without ambiguity to the commonly used circular slot in coaxial fixtures [3,6,14] when the frequency is low enough to assume that the current density and voltage have no azimuthal variation. (The TEM mode is dominant, and higher-order modes are negligible.) For straight slots, we can select a position (such as the slot center) at which to define the slot voltage. To simplify the discussion for straight slots, we assume that the current density and voltage are uniform along the slot. (This assumption is not rigorous, but it is approximately equivalent to a rigorous method using averages along the slot length.) For a slot length L, we can rewrite eq (29) as

$$Z_t = \frac{V_2}{LJ^i} = \frac{Z_{t2}}{L} = \frac{1}{LY_{12}}, \tag{30}$$

where Z_{t2} and Y_{12} were defined previously for the infinitely long slot.

It is instructive to consider the transmitted fields and power for the three-dimensional geometry shown in figure 3. We replace the slot by its equivalent magnetic current K(z') which initially is assumed to be a function of position z'. The plane x = 0 is a perfect conductor, and we wish to derive an expression for the far field radiated in the half space, x > 0. The electric field has only a ϕ component E_ϕ which for large $k_0 r$ is given by

$$E_\phi = \frac{-jk_0 \sin\theta}{2\pi r} e^{-jk_0 r} \int_{-L/2}^{L/2} K(z') e^{jk_0 z' \cos\theta} dz', \tag{31}$$

where ϕ and θ are standard spherical coordinates. The denominator contains a factor of 2 rather than 4 because of the image contribution. If the particular form of K(z') were known, the integral in eq (31) could be evaluated analytically or numerically.

For the special case where we assume the slot voltage is constant, $K(z') = K_0$, the integral in (31) can be evaluated in closed form

$$E_\phi = \frac{-jk_0 K_0 L \sin\theta}{2\pi r} \frac{\sin[(k_0 L \cos\theta)/2]}{[(k_0 L \cos\theta)/2]} e^{-jk_0 r}. \tag{32}$$

The Poynting vector has only an r component S_r which is given by

$$S_r = \frac{|E_\phi|^2}{\eta_0} = \left(\frac{k_0 K_0 L \sin\theta}{2\pi r}\right)^2 \left(\frac{\sin[(k_0 L \cos\theta)/2]}{[(k_0 L \cos\theta)/2]}\right)^2, \tag{33}$$

where K_0 is assumed to be real.

For an electrically short slot, $k_0 L \ll 1$, eq (32) reduces to

$$E_\phi \approx \frac{-jk_0K_0L\sin\theta}{2\pi r} e^{-jk_0r}. \tag{34}$$

In a similar manner, the Poynting vector reduces to

$$S_r \approx \frac{1}{\eta_0} \left(\frac{k_0K_0L\sin\theta}{2\pi r}\right)^2. \tag{35}$$

The total radiated power P_r can be obtained by integrating the Poynting vector over a hemisphere:

$$P_r = r^2 \int_0^{\pi}\int_0^{\pi} S_r \sin\theta \, d\theta \, d\phi. \tag{36}$$

In general the double integral in eq (36) must be evaluated numerically, but for the short slot Poynting vector in eq (35) the radiated power is

$$P_r = \frac{(k_0K_0L)^2}{3\pi\eta_0}. \tag{37}$$

In this case the radiated power is proportional to the square of the slot length which is analogous to short dipole radiation where the radiated power (or radiation resistance) is proportional to the square of the length.

3.2 Long Slots

For electrically long slots, eq (31) for E_ϕ is still valid, but the magnetic current (or slot voltage) $K(z')$ is not expected to be constant. From eq (31), we can write the square of the magnitude of the far electric field as

$$|E_\phi|^2 = \left(\frac{k_0 \sin\theta}{2\pi r}\right)^2 \int_{-L/2}^{L/2} \int_{-L/2}^{L/2} K(z')K^*(z'')\, e^{jk_0(z'-z'')\cos\theta}\, dz'dz'', \qquad (38)$$

where * indicates complex conjugate.

For long slots (large k_0L), the variation of $K(z')$ is likely to be complex and probably will not be known. In such cases it is probably best characterized by a random variable. This representation is also a good representation of reverberation chamber excitation [2,5] where the incident field is best represented as a random variable [15]. When $K(z')$ is a random variable, the expected value (indicated by $< >$) of eq (38) is

$$\langle|E_\phi|^2\rangle = \left(\frac{k_0 \sin\theta}{2\pi r}\right)^2 \int_{-L/2}^{L/2} \int_{-L/2}^{L/2} \langle K(z')K^*(z'')\rangle e^{jk_0(z'-z'')\cos\theta}\, dz'dz''. \qquad (39)$$

The expectation value $\langle K(z')K^*(z'')\rangle$ is not generally known. However, to obtain a simple result for the double integral in eq (39), we can make a simple incoherent assumption of the following form for the expectation:

$$\langle K(z')K^*(z'')\rangle = K_0^2\, \ell_c\, \delta(z' - z''), \qquad (40)$$

where K_0 is real, ℓ_c is a correlation length, and δ is the Dirac delta function. We choose the delta function rather than a more realistic peaked, finite function in eq (40) because it facilitates the evaluation of eq (39). The correlation length ℓ_c can be thought of as the width of an actual correlation function.

If we substitute eq (40) into eq (39) and evaluate the double integral, we obtain

$$\langle|E_\phi|^2\rangle = \left(\frac{k_0 K_0 \sin\theta}{2\pi r}\right)^2 \ell_c L. \qquad (41)$$

The expectation value of the Poynting vector is

$$\langle S_r \rangle = \langle |E_\phi|^2 \rangle / \eta_0 = \left(\frac{k_0 K_0 \sin\theta}{2\pi r}\right)^2 \frac{\ell_c L}{\eta_0}. \tag{42}$$

The expectation of the total radiated power is

$$\langle P_r \rangle = r^2 \int_0^{\pi} \int_0^{\pi} \langle S_r \rangle \sin\theta \, d\theta \, d\phi = \frac{k_0^2 K_0^2 \ell_c L}{3\pi\eta_0}. \tag{43}$$

The difference between eqs (43) and (37) is that eq (43) contains the factor $\ell_c L$ rather than L^2. This is consistent with Quine's conclusion [16] that the power radiated from a gasket at microwave frequencies is proportional to the length L of the gasket.

We can pursue Quine's gasket characterization [16] further. Since K_0^2 is equal to the square of a voltage, we can write it as the product of the square of the incident current density and the square of a transfer impedance of the type defined in eq (13):

$$K_0^2 = |J^i|^2 \, |Z_{t2}|^2. \tag{44}$$

We can replace the incident current by either the incident magnetic field H_0 or the magnitude of the incident Poynting vector S^i:

$$K_0^2 = 4H_0^2 |Z_{t2}|^2 = 4S^i |Z_{t2}|^2 / \eta_0. \tag{45}$$

If we substitute eq (45) into eq (43), we obtain

$$\frac{\langle P_r \rangle}{LS^i} = \frac{4k_0^2 \ell_c |Z_{t2}|^2}{3\pi\eta_0^2}. \qquad (46)$$

Equation (46) provides an analytical expression for Quine's effective transmission area (ETA) per unit length [16] which he proposed for gasket characterization (by measurement) at microwave frequencies. It has dimensions of length.

4. GASKET MEASUREMENTS

4.1 Measurement Geometries

The specific measurement fixture or geometry depends on what quantity is being determined. Transfer impedance and shielding effectiveness are the most commonly measured gasket characteristics.

A circular coaxial fixture [3,6,14] has typically been used to measure transfer impedance. A current is made to flow from the center conductor across the circular gasketed slot to the shield, and the voltage between the center conductor and the shield on the other side of the gasketed slot is measured. The transfer impedance is the ratio of the measured voltage to current. The method is normally considered to be applicable for frequencies where only the TEM mode is supported by the coaxial structure [6]. At frequencies where higher modes can propagate, the current and voltage are not necessarily uniform around the circumference of the coaxial fixture. For example, Freyer and Hatfield [17] found resonances due to higher-order modes above 2 GHz, and Carlson and Kasevich [18] found resonances (not necessarily due to higher-order modes) above 200 MHz. Kunkel [3] reported on a coaxial fixture that is free of resonances up to 10 GHz, but Freyer and Hatfield [17] and Adams [4] found resonances above 2 GHz with the same fixture.

In theory a circular coaxial fixture can also be used to measure shielding effectiveness. This requires an additional measurement of

received power without the gasket in place. Shielding effectiveness is then determined by the ratio of received power without and with the gasket in place. Adams [4] performed SE measurements using a modification of the ASTM coaxial fixture that was originally designed for measuring SE of planar materials. If no reference is made, SE can be calculated from the transfer impedance of a coaxial fixture by making a circuit-model assumption [4,5].

For radiated excitation of gaskets, SE measurements have been performed using either a shielded enclosure [1] or nested reverberation chambers [19]. The military standard, MIL-G-83528, uses a large square hole (60 cm by 60 cm) cut in the wall of a shielded enclosure with two high-gain antennas aimed at each other through the hole to obtain a reference reading. The hole is then covered up with a gasketed cover to obtain a second reading. The ratio of the two readings is called the shielding effectiveness of the gasket. The main problem with the method is that the standing waves that typically occur inside shielded rooms make the results a strong function of the position of the antenna. The nested reverberation chamber method [19] requires a mechanical stirrer and an antenna within each nested cavity. A reference value is taken with a large hole in the interior cavity, and a second reading is taken with a gasketed cover in place. The ratio of the two readings represents an average over all incidence angles and polarizations. The mode stirring makes the method insensitive to antenna positions, but the method requires more extensive data taking.

In both of the above methods, the open hole reference (rather than open slots) raises a question. Are the methods measuring SE of the gasket or the gasketed cover? For a relative comparison of two different gaskets, the question is unimportant. However, if we accept the IEEE definition of shielding effectiveness ("the ratio of electric or magnetic field strength at a point before and after the placement of the shield in question"), then the two methods are clearly measuring SE of the gasketed cover.

4.2 Measured Data

In this section we compare trends of the measured data reported in the literature with the theory in this report. Only trend comparisons are

possible because the precise parameters of the gaskets or slots are seldom given, and the fixture geometries do not generally fit idealized models.

Hoeft and Hofstra [20] performed a number of shielding measurements on a box located inside a TEM cell. Their data showed a variety of frequency dependencies, but generally the attenuation showed an attenuation increase with frequency of 10 to 20 dB/decade. The description of the box construction indicated that field penetration was through joints or very narrow slots. For very narrow slots (thin air gaps), the limiting form of the transfer impedance Z_{t2} in eq (25) is applicable. The k_0 factor in the denominator would produce a 20 dB/decade increase in shielding (decrease in slot voltage). The slowly varying $\ell n(k_0 w)$ factor would make the actual rate of increase somewhat less. If skin depth penetration were the actual physical mechanism, then the approximation of Z_{t2} in eq (23) would yield an exponential decrease in $|Z_{t2}|$ multiplied by a square root factor. This decrease in $|Z_{t2}|$ with frequency at least produces a change in attenuation in the right direction (an increase) with frequency. In a separate measurement of joint impedance, Hoeft and Hofstra [20] obtained a square root dependence on frequency which is consistent with the skin depth approximation of slot impedance Z_2 in eq (24).

Faught [14] measured the transfer impedance of a number of gasket materials in a coaxial fixture for frequencies from 0.1 to 1000 MHz. Most of his low frequency data show a constant transfer impedance which is consistent with the low-frequency limit for a lossy material as given by eq (18). Most of his higher frequency data show a slow decrease in transfer impedance with frequency which is consistent with air-gap theory as given by eq (25). However, one knitted gasket shows an increase in transfer impedance with frequency, and this appears to be consistent with small-aperture theory as described by aperture polarizability [21]. In all cases, his data show a decrease in transfer impedance with an increase in pressure, indicating that the pressure should be carefully controlled in gasket measurements. Kunkel's measured data for transfer impedance show a slow decrease with frequency which is also consistent with air-gap theory as given by eq (25). Most of Madle's measured data [6] for transfer impedance

show an increase with frequency, and this appears to be because his gaskets contained small apertures as with mesh or honeycomb.

The most comprehensive attempt at characterizing gaskets by different methods [5] included a shielded room with an aperture [1], nested reverberation chambers [20], a coaxial transfer impedance fixture [3], and a modified ASTM coaxial holder [3]. The discouraging lack of agreement between the four methods on several gaskets is best described by quoting from [5]: "The results indicate little consistency between measurement techniques for: establishing the relative order of the gaskets by shielding performance; determining the magnitude of the shielding performance for a given gasket; and defining the frequency dependence of the shielding performance of a gasket." Part of the difficulty is perhaps that the four different methods employ different fixtures with different geometries, and there is nothing that can be done about that. However, another difficulty could be that none of the four methods as performed in [5] uses a reference measurement in the absence of the gasket only. Both the shielded room [1] and the nested chamber methods remove both the gasket and aperture cover, and the coaxial fixture for measuring transfer impedance [3] does not use a reference measurement. The modified ASTM coaxial fixture [4] can be used to take a reference measurement with no gasket, but that was not done in [5].

Kunkel [22] performed a set of measurements on slots and gaskets of different length where he recorded both slot voltage and radiated electric and magnetic fields for frequencies up to 50 MHz. Good correlation between slot voltage and transmitted electric or magnetic field was found in all cases which indicates that slot voltage (proportional to transfer impedance) is a good indicator of shielding effectiveness for thin slots and gaskets. This also indicates that the magnetic line source model in section 3.1 should be a good predictor of radiated fields. However, the measurements at higher frequencies (4.0, 6.0, and 8.0 GHz) by Quine et al. [23] show significant variability in the radiated fields due to variations along the gasket length. Consequently, they conclude that high-frequency gasket performance is best measured in a reverberation chamber via a total radiated power measurement. This is consistent with the theory for long gaskets with statistical variation in section 3.2.

5. CONCLUSIONS AND RECOMMENDATIONS

An idealized two-dimensional model for a uniform gasket in a uniform slot reveals that a transfer impedance with units of Ω•m is a valid characterization of a uniform gasket. The units result from a ratio of slot voltage (V) to surface current density (A/m). For a real gasket of finite length, the transfer impedance is a ratio voltage to current and has units of Ω. The ratio between the three-dimensional and two-dimensional transfer impedances is not necessarily equal to the gasket length because the voltage and current density may not be constant along the gasket. A coaxial fixture that is electrically small can possibly maintain constant voltage and current density around the gasket circumference, but even then the effects of curvature and fixture geometry are uncertain. For example, Kunkel's transfer impedance fixture [3] and Adam's modified ASTM coaxial holder [4] have different geometries and have given substantially different results for the same gaskets [5].

For electrically long gaskets, it is unlikely that any simple per-unit-length property will give a complete description. The slot voltage and current density are typically nonuniform because either the incident current density or the gasket properties (including contact impedance) will vary over the gasket length. The idealized statistical theory in section 3.2 is consistent with Quine's effective transmission area (ETA) per unit length [16]. Both descriptions are consistent with nested reverberation chamber measurements [19]. Although shielding effectiveness (SE) is a natural description of gaskets, most methods do not use a valid reference measurement where only the gasket is removed. This makes it very difficult to compare the same gasket with different measurement methods and results in very different SE values for the same gasket [5]. The difficulty of controlling the gasket pressure [14] from one fixture to another is probably another source of variability.

Even if the transfer impedance characterization as measured by a coaxial fixture at low frequencies and either SE or ETA as measured by nested reverberation chambers at high frequencies are valid, a question remains on the appropriate frequency range for each characterization. It would be useful to do a careful study on a simple geometry, such as a single

straight slot, to determine the frequency range of validity of the different characterizations. The time-domain method which uses transmission through thin sheets for SE measurements of material sheets [24] could be used for gasket measurements. The time windowing of edge effects would eliminate the problems caused by placing one antenna in a shielded room [1]. The broadband information would be useful for obtaining the frequency dependence of SE quickly, and the reference measurement could be the empty slot without the gasket. The same metal sheet could be used in a nested reverberation chamber measurement of SE [19] to study the equivalence of the two methods at high frequencies. Using the same slot and gasket in both measurements might help to provide better agreement between the two methods than has been obtained using significantly different fixtures [5]. The comparison would also provide further study of the issue of transmission in a single direction normal to the slot versus the total radiated power over all angles [24]. A computational study, perhaps by FDTD [25], of the slot geometry with and without a gasket would also help to add to the understanding to the experimental results.

6. REFERENCES

[1] Military Standard MIL-G-83528B, July 1992.

[2] Hatfield, M.O. Shielding effectiveness measurements using mode-stirred chambers: a comparison of two approaches. IEEE Trans. Electromag. Compat., 30: 229-238; 1988.

[3] Kunkel; G.M. Design of transfer impedance test fixture accurate through 10 GHz. IEEE International EMC Symposium: 628-633; 1990.

[4] Adams, J.W. Electromagnetic shielding of rf gaskets by two methods. IEEE International EMC Symposium: 154-157; 1992.

[5] Freyer, G.J.; Rowan, J.; Hatfield, M.O. Gasket shielding performance measurements obtained from four test techniques. IEEE International EMC Symposium: 279-284; 1994.

[6] Madle, P.J. Transfer impedance and transfer admittance measurements on gasketed panel assemblies, and honeycomb air-vent assemblies. IEEE International EMC Symposium: 204-209; 1976.

[7] Harrington, R.F.; Auckland, D.T. Electromagnetic transmission through narrow slots in thick conducting screens. IEEE Trans. Antennas Propagat., AP-28: 616-622; 1980.

[8] Auckland, D.T.; Harrington, R.F. Electromagnetic transmission through a filled slit in a conducting plane of finite thickness, TE case. IEEE Trans. Microwave Theory Tech., MTT-26: 499-505; 1978.

[9] Lee, K.S.H., editor. EMP Interaction: Principles, Techniques, and Reference Data. Santa Monica: Hemisphere Pub. Corp.; 1986.

[10] Warne, L.K.; Chen, K.C. Relation between equivalent antenna radius and transverse line dipole moments of a narrow slot aperture having depth. IEEE Trans. Electromag. Compat., 30: 364-370; 1988.

[11] Warne, L.K.; Chen, K.C. Equivalent antenna radius for narrow slot apertures having depth. IEEE Trans. Antennas Propagat., 37: 824-834; 1989.

[12] Warne, L.K.; Chen, K.C. Slot apertures having depth and losses described by local transmission line theory. IEEE Trans. Electromag. Compat., 32: 185-196; 1990.

[13] Warne, L.K.; Chen, K.C. A simple transmission line model for narrow slot apertures having depth and losses. IEEE Trans. Electromag. Compat., 34: 173-182; 1992.

[14] Faught, A.N. An introduction to shield joint evaluation using EMI gasket transfer impedance data. IEEE International EMC Symposium: 38-44; 1982.

[15] Hill, D.A.; Crawford, M.L.; Kanda, M.; Wu, D.I. Aperture coupling to a coaxial air line: theory and experiment. IEEE Trans. Electromag. Compat., 35: 69-74; 1993.

[16] Quine, J.P. Characterization and testing of shielding gaskets at microwave frequencies. IEEE International EMC Symposium: 306-308; 1993.

[17] Freyer, G.J.; Hatfield, M.O. Comparison of gasket transfer impedance and shielding effectiveness measurements, part I. IEEE International EMC Symposium: 139-141; 1992.

[18] Carlson, E.J.; Kasevich, R.S. Analysis of transfer impedance technique: equivalent circuit model and network analyzer measurements. IEEE International EMC Symposium: 1-6; 1987.

[19] Hatfield, M.O.; Freyer, G.J. Comparison of gasket transfer impedance and shielding effectiveness measurements, part II. IEEE International EMC Symposium: 142-148, 1992.

[20] Hoeft, L.O.; Hofstra, J.S. Experimental and theoretical analysis of the magnetic field attenuation of enclosures. IEEE Trans. Electromag. Compat., 30: 326-340; 1988.

[21] Butler, C.M.; Rahmat-Samii, Y.; Mittra, R. Electromagnetic penetration through apertures in conduction surfaces. IEEE Trans. Antennas Propagat., AP-26: 82-93; 1978.

[22] Kunkel, G.M. Electromagnetic leakage through slot configurations in a shielded enclosure. IEEE International EMC Symposium: 274-278; 1994.

[23] Quine, J.P.; Pesta, A.J.; Streeter, J.P.; Surowic, E.A. Distortion of radiation patterns for leakage power transmitted through attenuating cover panels and shielding gaskets -- need for reverberation chamber measurement of total leakage power. IEEE International EMC Symposium: 285-290; 1994.

[24] Wilson, P.F.; Ma, M.T. A study of techniques for measuring the electromagnetic shielding effectiveness of materials. Nat. Bur. Stand. (U.S.) Tech. Note 1095; 1986.

[25] Kunz, K.L.; Luebbers, R.J. The Finite Difference Time Domain Method for Electomagnetics. Boca Raton: CRC Press; 1993.

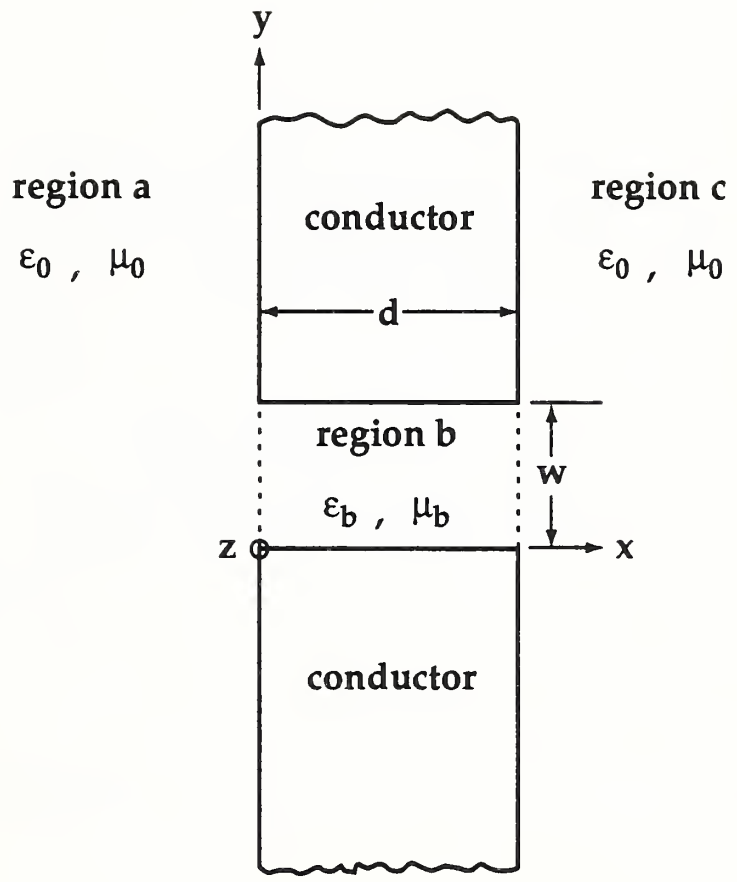

Figure 1. Two-dimensional geometry for a slot in a thick screen filled with gasketing material.

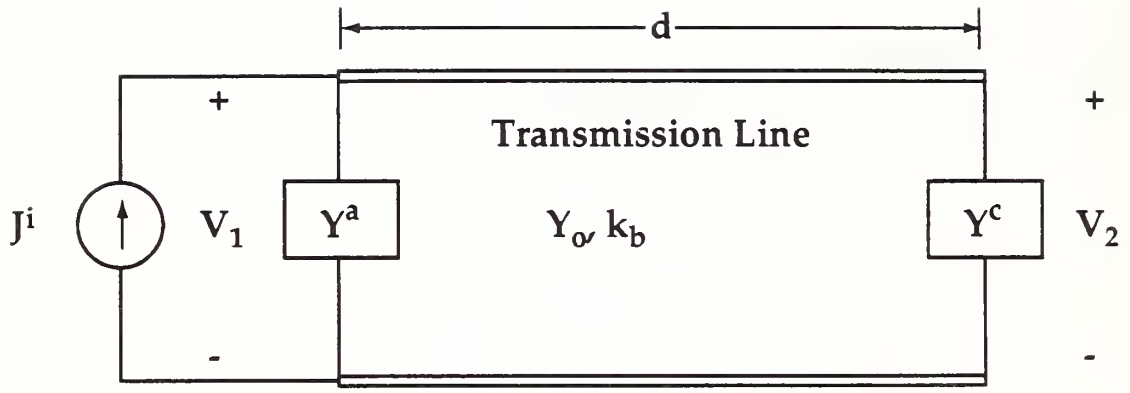

Figure 2. Equivalent circuit for a narrow slot in a thick screen excited by surface current.

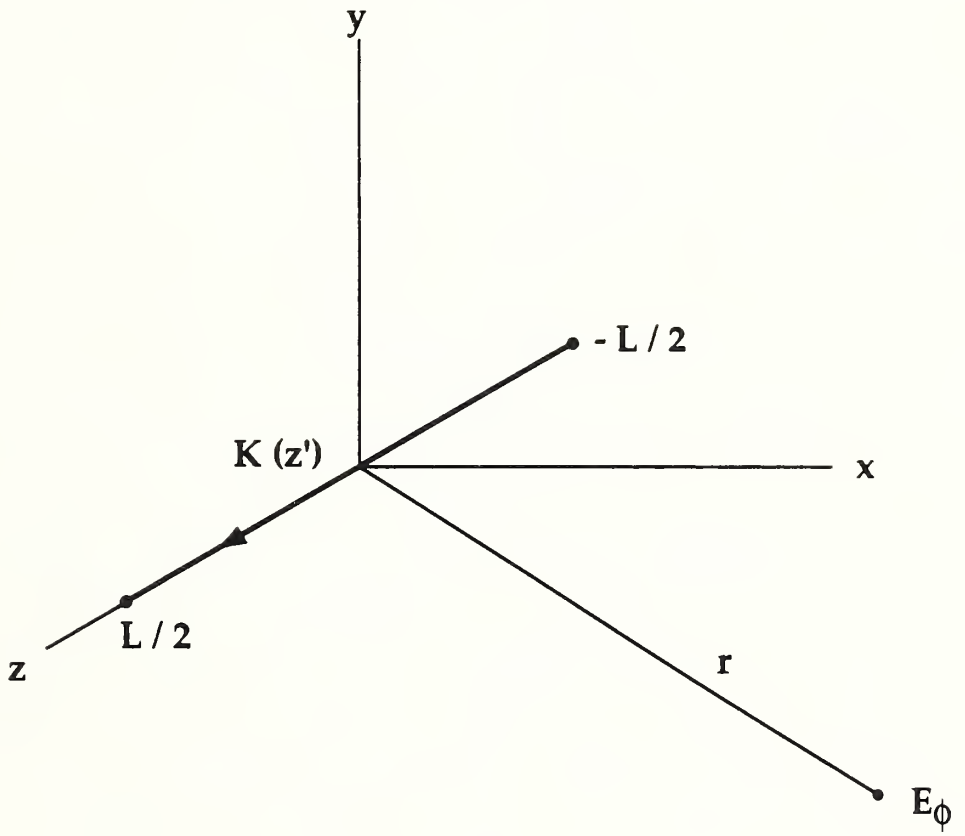

Figure 3. Equivalent magnetic line current K of finite length L radiating into the half space, x > 0.